

Natural Convection in a Square Cavity: Numerical Study for Different values of Prandtl Number

ADNANI Massinissa¹, MEZIANI Bachir², OURRAD Ouerdia² and ZITOUNE Mounir¹

Abstract A numerical study of natural convection in a square cavity subjected to the thermals boundary conditions on the sidewalls is presented and discussed. The fluid is Newtonian and equations governing the flow field and the heat transfer are given in dimensionless form. The finite volume method was adopted to solve the algebraic system. Influence of the Prandtl and the Rayleigh numbers on heat transfer and the flow field is illustrated and discussed as the stream functions, isotherms, horizontal velocity, local and average Nusselt numbers. Results indicate that improved heat transfer is more pronounced with increasing Rayleigh number. In particular, at low Rayleigh numbers, the flow field is slightly pronounced with increasing Prandtl number and decreases by increasing the Rayleigh number. In contrast, the heat transfer is not affected by variations of Prandtl number at low Rayleigh numbers and decrease with increasing the Prandtl number especially for very high Rayleigh numbers.

Keywords: Natural convection, square cavity, boundary conditions, finite volume method.

Nomenclature

g	gravitational acceleration, $m\ s^{-2}$
H	cavity height, m
Nu_{Local}	local Nusselt number along the haut walls
Nu	average Nusselt number
P	dimensionless pressure
Ra	Rayleigh number
Pr	Prandtl number
T	Temperature, K
U, V	dimensionless velocity components
u, v	velocity components, $m\ s^{-1}$
X, Y	dimensionless cartesian coordinates
x, y	cartesian coordinates, m

¹ Laboratoire de Physique Théorique, Faculté de Technologie, Université de Bejaia, 06000, Algérie.

² Laboratoire de Physique Théorique, Faculté des Sciences Exactes, Université de Bejaia, 06000, Algérie.

Corresponding author: M.ADNANI, Email: massinissa.adnani@univ-bejaia.dz

Greek Symbols

μ	dynamic viscosity, Pa.s
ρ	mass density, kg/m ³
α	thermal diffusivity, m ² s ⁻¹
β	coefficient of thermal expansion, K ⁻¹
Ψ	dimensionless stream function
θ	dimensionless temperature

Subscripts

c	cold
h	hot
max	maximum values
local	local values

1 Introduction

Natural convection that develops in a closed cavity finds applications in many fields. We quote thermal power, petrochemical industries, aerospace and construction. Several studies have been conducted to understand this phenomenon. A numerical study of laminar natural convection in a rectangular and square cavity was carried and discussed by [De Vahl Davies (1968, 1983)]. An analytical study was presented by Misici (1984). The sensibility of fluid properties, namely the effect of the Prandtl number, on the natural convection widely documented by [Lage, Bejan, and Georgiadis (1991); Bejan, Georgiadis (1992)]. [Yoo (1999)] investigated transition of free-convective flows in a wide-gap horizontal annulus. They found that bifurcation points are functions of the Prandtl number. [Poujol, Rojas and Ramos (2000)] analyzed the natural convection problem in a square cavity for high Prandtl number. It happens that the natural convection quantitatively and qualitatively depends on the combination of the boundary conditions imposed on the walls, as well as the position of the cavity with respect to the gravity center [Cianfrini, Corcione, and Dell’Omo (2005); Basak, Roy, and Balakrishnan (2006); Corcione, (2003); Huelez, Rechtman (2013)]. Buoyancy forces entrained by temperature gradients tend to increase heat transfer and natural convection pronounces increasingly with increasing temperature gradient. [Mahmoudi, (2011); Sadaoui, Sahi, Hamici, Meziani and Amoura (2015)] have conducted numerical studies on natural convection in square cavities in the presence of a thin plate subjected to a hot temperature inside the enclosure. They examined the effect of the plate on the heat transfer and the flow field. The heat transfer depends essentially on the geometry and position of the plate. Thus, the heat transfer is more pronounced with increasing Rayleigh number.

[Aminossadati, Ghasemi and Kargar (2014)] have studied laminar natural convection in a square cavity with a thin fin under the influence of a uniform magnetic field. Results indicate that, at higher Rayleigh numbers, the flow and temperature fields and the heat transfer rate of the cavity are all influenced by the magnetic field. [Oztop, Zaiguo, Bo and Wei (2011)] performed a numerical study of fluid flow and heat transfer due to buoyancy forces in a tube inserted in a square cavity filled with fluid. The results indicate that the

heat transfer and the flow field depend on the position of the inserted tube and are affected by the variation of the Rayleigh number.

Regarding the numerical associated with experimental studies, heat transfer by natural convection and thermal radiation on a solar open cubic cavity- type receiver, studied by [Montiel, Hinojosa, Villafan, Bautista and Estrada (2015)], show that experimental and theoretical results comparison is better when using model with variable thermophysical properties than Boussinesq approximation. [Nardini and Paroncini (2012)] investigate effects of the different sizes and positions of the heat sources on the natural convective heat transfer. A comparison between the experimental data and numerical data presents a good level of agreement for the Rayleigh numbers ranging from 10^4 to 10^5 . Development of the natural convection heat transfer increase with increasing Rayleigh numbers and the velocity field is influenced by the size and the positions of the heat sources. Other studies are focused on the triangular geometry. [Mahmoudi, Mejri, Abassi and Omri (2013)] carried a numerical study of natural convection in an inclined triangular cavity for different thermal boundary conditions and observed that the heat transfer mainly depends on the inclination angle. [Koca, Oztop and Varol (2007)] conducted a numerical study of natural convection in triangular enclosures. Results showed that both flow and temperature fields are affected with the changing of Prandtl number, location and length of heater as well as Rayleigh number. For cylindrical cavity, natural convection heat transfer from a heated horizontal semi-circular cylinder has been investigated by [Chandra and Chhabra (2012)]. They have developed predictive correlations to estimate Nusselt number value based on Prandtl and Grashof numbers in a new application. Cavity heated through the side walls at low Prandtl numbers with large density differences has been investigated numerically and theoretically by [Pesso and Piva (2009)]. Analysis indicate that the heat transfer increases with the Prandtl number, particularly, for very high Rayleigh numbers. At last, three dimensional numerical investigation of natural convection in an isothermal open cavity were presented by [Hinojosa and Cervantes-de Gortari (2010)].

All these works clarify a set of physical phenomena observed in natural convection in cavities. To provide further clarifications, we analyze the effect of boundary conditions imposed on the side walls of the cavity for different values of Rayleigh and Prandtl numbers.

2 Mathematical formulation

2.1 Problem description

We considered a square cavity, filled with a Newtonian fluid. As shown in Fig.1, the upper and lower horizontal walls are kept adiabatic. The side walls are composed of two parts of the same dimension, the lower half of the side walls is maintained at a hot temperature and the upper half is maintained at a cold temperature. The X axis is parallel to the adiabatic walls, the Y axis is parallel to the side walls and the gravity is directed downwardly.

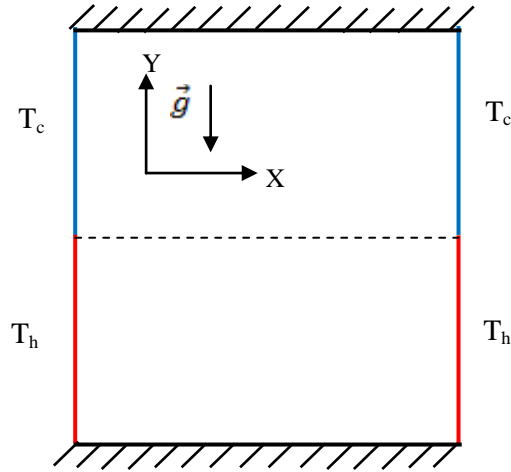


Figure 1 : Physical model.

2.2 Governing equations

To model the problem, we consider the two-dimensional steady laminar flow of an incompressible Newtonian fluid. Transfers by radiation are negligible, viscous dissipation is neglected in the energy equation and Boussinesq approximation is adopted.

Considering the following dimensionless variables:

$$X = \frac{x}{H}; Y = \frac{y}{H}; U = u \frac{H}{\alpha}; V = v \frac{H}{\alpha}; \theta = \frac{T - T_c}{T_h - T_c}; P = \frac{pH^2}{\rho\alpha^2} \quad (1)$$

We take into account assumptions cited with introduction of the dimensionless variables, the dimensionless continuity, momentum and energy equations are written as follows:

$$\frac{\partial U}{\partial X} + \frac{\partial V}{\partial Y} = 0 \quad (2)$$

$$U \frac{\partial U}{\partial X} + V \frac{\partial U}{\partial Y} = -\frac{\partial P}{\partial X} + \text{Pr} \left(\frac{\partial^2 U}{\partial X^2} + \frac{\partial^2 U}{\partial Y^2} \right) \quad (3)$$

$$U \frac{\partial V}{\partial X} + V \frac{\partial V}{\partial Y} = -\frac{\partial P}{\partial Y} + \text{Pr} \left(\frac{\partial^2 V}{\partial X^2} + \frac{\partial^2 V}{\partial Y^2} \right) + Ra \text{Pr} \theta \quad (4)$$

$$U \frac{\partial \theta}{\partial X} + V \frac{\partial \theta}{\partial Y} = \left(\frac{\partial^2 \theta}{\partial X^2} + \frac{\partial^2 \theta}{\partial Y^2} \right) \quad (5)$$

$\text{Pr} = \frac{\mu}{\rho\alpha}$ and $Ra = \frac{g\beta(T_c - T_f)\rho^2 H^3 \text{Pr}}{\mu^2}$ are the Prandtl and Rayleigh numbers, respectively.

Considering no slip condition at the walls, the dimensionless boundary conditions are:

$$\begin{aligned}
U(X, 0) = U(X, 1) = U(0, Y) = U(1, Y) = 0 \\
X = 0, X = 1, 0 \leq Y \leq 0.5, \theta = 1 \\
X = 0, X = 1, 0.5 \leq Y \leq 1, \theta = 0 \\
0 \leq X \leq 1, \left. \frac{\partial \theta}{\partial Y} \right|_{Y=0} = \left. \frac{\partial \theta}{\partial Y} \right|_{Y=1} = 0
\end{aligned} \tag{6}$$

The fluid motion is displayed using the stream function obtained from the velocity components U and V. The relationships between the stream function and the velocity components for two-dimensional flows are:

$$U = \frac{\partial \psi}{\partial Y} \text{ and } V = -\frac{\partial \psi}{\partial X} \tag{7}$$

Which yield to a single equation:

$$\frac{\partial^2 \psi}{\partial X^2} + \frac{\partial^2 \psi}{\partial Y^2} = \frac{\partial U}{\partial Y} - \frac{\partial V}{\partial X} \tag{8}$$

Nusselt number is one of the most important dimensionless parameters in describing the convective heat transport. The local Nusselt number at the hot wall calculated as:

$$Nu_{Local} = \left(-\frac{\partial \theta}{\partial X} \right) \Big|_{X=0} + \left(-\frac{\partial \theta}{\partial X} \right) \Big|_{X=1} \tag{9}$$

The average Nusselt number on the hot walls is given by:

$$Nu = \int_0^{0.5} \left(-\frac{\partial \theta}{\partial X} \right) \Big|_{X=0} dY + \int_0^{0.5} \left(-\frac{\partial \theta}{\partial X} \right) \Big|_{X=1} dY \tag{10}$$

3 Procedure and numerical validation

Eqs. (2)-(5) are integrated on control volumes in order to obtain an algebraic equation system more accessible to the resolution [Patankar (1980)]. The SIMPLE algorithm is used to solve the coupled system of algebraic equations. Spatial discretization of the continuity, momentum and energy equations is done by a second order upwind scheme. The interpolation of the pressure is carried out by the PRESTO scheme. The calculation is performed using the commercial finite volume code FLUENT. To check the convergence of the sequential iterative solution, normalized residual respectively for the continuity, momentum and energy equation is calculated, convergence is obtained when the residual becomes smaller than 10^{-9} .

3.1 Grid independence study

In order to determine a proper grid for the numerical simulation, a square cavity filled with air, Pr = 0.71 at Ra = 105 is chosen. Eight different uniform grids, namely, 51X51, 61X61, 81X81, 101X101, 121X121, 141X141, 161X161 and 181 X181 are employed for the numerical simulation. The average Nusselt number on the hot side walls and the maximum of the stream function for these grids are shown in Table 1. As can be

observed from the table, a uniform 121X121 grid is sufficiently fine for the numerical calculation. This grid gives the best compromise between cost and accuracy calculations.

Table 1: Grid independence results ($Pr = 0.71$ and $Ra = 10^5$)

Grid	51X51	61X61	81X81	101X101	121X121	141X141	161X161	181X181
Nu	4.2038	4.3175	4.5005	4.6442	4.7621	4.8620	4.9485	5.0249
Ψ_{\max}	0.4962	0.4955	0.4941	0.4935	0.4933	0.4930	0.4930	0.4930

3.2 Code validation

To validate the proposed numerical scheme, the steady of laminar natural convection flow in a square cavity with uniformly heated bottom wall and adiabatic top wall maintaining constant temperature of cold vertical walls is analyzed using the presented code, and the results are compared with the results of [Basak, Roy, and Balakrishnan (2006)] for the same problem. Fig. 2 shows the local Nusselt number of heated bottom wall obtained by the present simulation and the results of [Basak, Roy, and Balakrishnan (2006)]. Another comparison was mad with cavity heated from the left wall and cooled from the right isothermally and horizontal walls were adiabatic using the presented code, and the result are compared with the results of [De Vahl Davies (1983); Hortmann, Peric and Scheuerer (1990)]. Tab. 2 shows the average Nusselt number of the left wall obtained by the present simulation and the results of [De Vahl Davies (1983); Hortmann, Peric and Scheuerer (1990)]. As can be observed from the Fig.2 and the Tab. 2, very good agreements exist between our results and those given by the references which justified the accuracy of our numerical results.

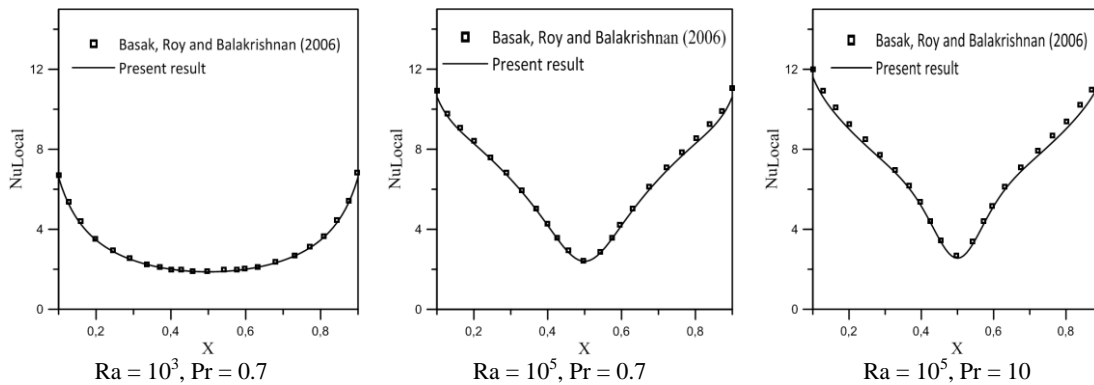


Figure 2: Comparison between our results and those of [Basak, Roy, and Balakrishnan (2006)] for local Nusselt number of heated bottom wall

Table 2: Comparison between our results and those of [De Vahl Davies (1983); Hortmann, Peric and Scheuerer (1990)] for average Nusselt number

Ra	Nu(this study)	Nu (De Vahl Davies (1983))	Nu (Hortmann, Peric and Scheuerer (1990))
10^5	4.53	4.50	4.55
10^6	8.92	9.035	9.00

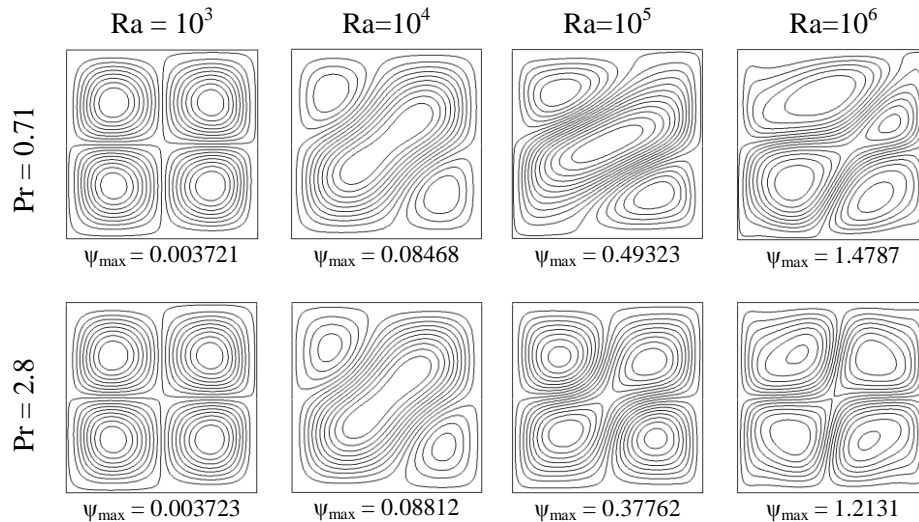
4 Results and discussion

In order to see the influence of the parameters governing the flow field and heat transfer on natural convection, the variations of the Rayleigh number ($10^3 \leq Ra \leq 10^6$) and Prandtl number ($0.71 \leq Pr \leq 7$) are illustrated and discussed. The results are given in the form of streamlines, isotherms, horizontal velocity, local and average Nusselt number.

The flow fields given by the streamlines are shown in Fig.3 for different Rayleigh numbers ($10^3 \leq Ra \leq 10^6$) and Prandtl numbers ($0.71 \leq Pr \leq 7$).

For $Ra=10^3$, $Pr = 0.71$ to $Pr = 7$, four counter rotating cells and symmetrical with respect to the cavity axes plane (X, Y) appear. The stream functions are very low and a minimal increase of maximum stream functions (Ψ_{max}) noted when the Prandtl number becomes important. At $Ra = 10^4$, the flow near the central region of the cavity becomes more and more important. The two cells located on the diagonal tend to approach and form a large main cell rotating counterclockwise and the stream functions increase with increasing Prandtl number. Indeed, at low temperature gradients, the flow field is slightly pronounced with increasing Prandtl number.

When Rayleigh number increases up 10^5 , at $Pr = 0.71$, the flow is characterized by a strong circulation in the middle of the cavity and a large main cell rotating counterclockwise is formed on the diagonal enclosure with two small secondary cells occupy the high left and low right portions of the cavity rotating clockwise. When Prandtl number increases to $Pr=7$, the large main cell undergoes a deformation and a compression on the part the two cells located near the side walls which tend to return to their initial physical states with a high counterclockwise circulation. However, the opposite effect of Prandtl number on the maximum of stream functions is noted in this case ($Ra = 10^5$), so the maximum of the stream functions are less pronounced with increasing Prandtl number.



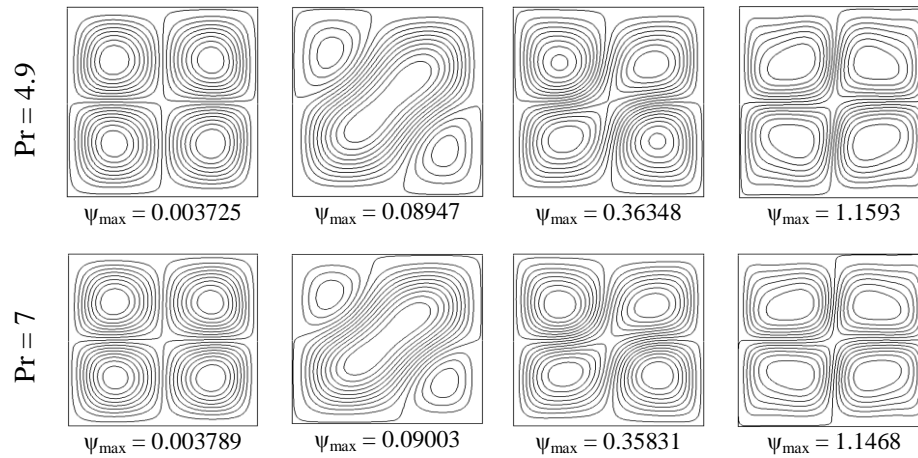


Figure 3: Rayleigh and Prandtl numbers effects on stream lines

At $Ra = 10^6$, considerable deformation of the stream functions is observed. For Prandtl number $Pr = 0.71$, the large cell is deformed into two cells occupying the diagonal part of the enclosure. These cells become more and more symmetric with respect to cavity plane axis and the maximum of the stream functions are less pronounced with increasing Prandtl number.

The heat transfer given by the isotherms is shown in Fig.4 for different values of Rayleigh number ($10^3 \leq Ra \leq 10^6$) and Prandtl number ($0.71 \leq Pr \leq 7$).

At $Ra = 10^3$, in all situations ($Pr = 0.71$ to 7), the isotherms occur symmetrically with respect to the cavity axis. Indeed, the isotherms are not affected by the variation of the Prandtl number and the heat transfer is mainly due to conduction. Furthermore, the isotherms begin to move toward the side walls and tend to deform when $Ra = 10^4$. In this case, the isotherms are slightly affected by the variations of the Prandtl number. As shown in Fig.4, when the Prandtl number increases up $Pr = 2.8$, the isotherms are shifted slightly toward the top and bottom walls, then, tend to invariant situations when the Prandtl number increases up $Pr = 7$. However, the heat transfer by natural convection becomes more and more important in the cavity center.

At $Ra = 10^5$ and 10^6 , more pronounced compression of the isotherms towards the side walls of the enclosure occurs. As shown in the figure, when the Prandtl number increases, the isotherms are attracted to the middle of the cavity central zone and tend towards an axial symmetry. Therefore, the opposite effect of Prandtl number is observed when the Rayleigh number becomes important, consequence of thermal effects that become very low in front of the viscous effects. In fact, the temperature gradient in the vicinity of the side walls becomes important for the development of a thermal boundary layer and the heat transfer corresponds to a natural convection.

Fig.5 show the horizontal velocity profiles in the middle of the cavity ($X = 0.5$, $Y = 0$ to 1) for $Ra = 10^3$ to 10^4 and $0.71 \leq Pr \leq 7$.

At $Ra = 10^3$, the flow is very low along this section of the cavity, the velocity tends to zero for $Pr = 0.7$ and an increase is noted for $Pr = 7$. Therefore, at low temperature gradients, the horizontal velocity profile seems slightly significant with increasing

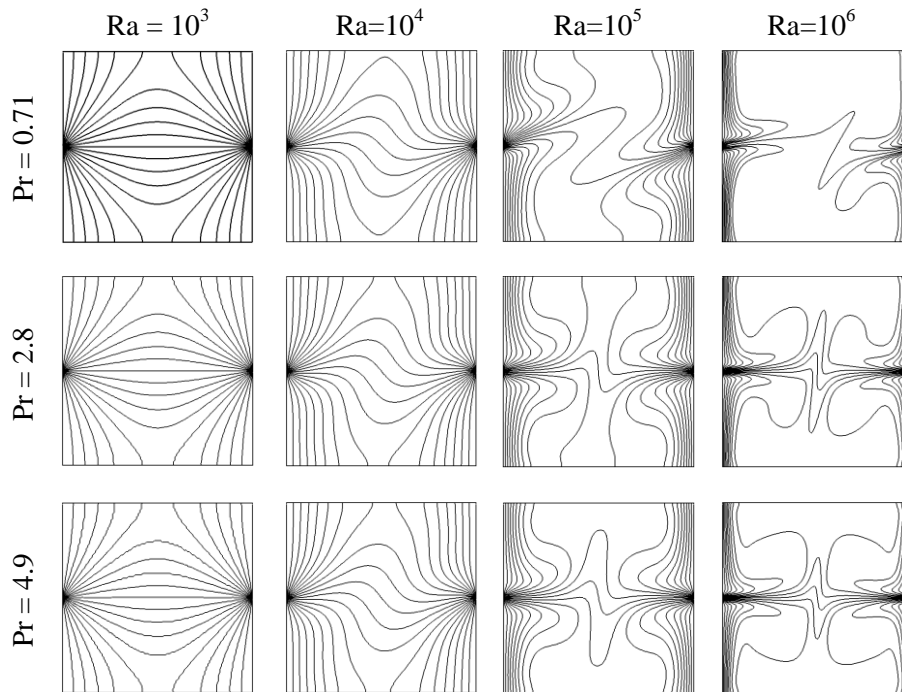
Prandtl number. Obviously, the flow velocity is more pronounced for Rayleigh number $Ra = 10^4$. As shown in the figure, symmetry of the flow can be seen with respect to the median cavity plane. Therefore, the velocity becomes important at the top and bottom of the cavity with a zero value in the middle.

In addition, the flow increases slightly with increasing Prandtl number at the top of the cavity and less pronounced at the bottom with identification in the middle of the cavity.

When $Ra = 10^5$ and $Ra = 10^6$, the flow becomes more significant when the Rayleigh number increases. However, there is a reverse effect of Prandtl number compared to the low temperature gradients. In this situation, the flow is less pronounced by increasing the Prandtl number. Therefore, the viscosity effects become more important as Prandtl increases which will result in the weakening of the flow field.

The heat transfer given by the local Nusselt number along the left hot wall is illustrated in Fig.6 for $Ra = 10^3$ to 10^6 and $Pr = 0.71$ to 7.

For $Ra = 10^3$, local Nusselt number undergoes exponential growth along the hot wall. When $Ra = 10^4$, the profiles of the Nusselt keep a substantially constant evolution along the wall until $Y = 0.7$ and then greatly increase. It is evident to note that in this situation the heat transfer is not affected by the Prandtl number, in particular for low values of the Rayleigh number and the heat transfer corresponds to the conduction. When Rayleigh number increases up $Ra = 10^5$, the Nusselt number increases significantly compared to the previous cases. Indeed, we note that the heat transfer is affected Prandtl number variations. In fact, at the extremities of the heated wall, heat transfer by conduction seems to dominate as seen from the growth of local Nusselt profiles. In this case, the heat transfer is less pronounced for Prandtl number equal to 0.71.



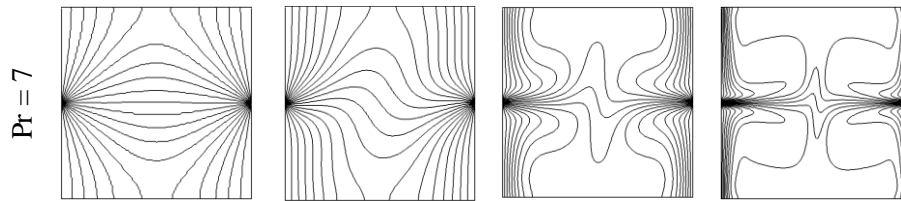


Figure 4: Effect of Rayleigh and Prandtl numbers on isotherm

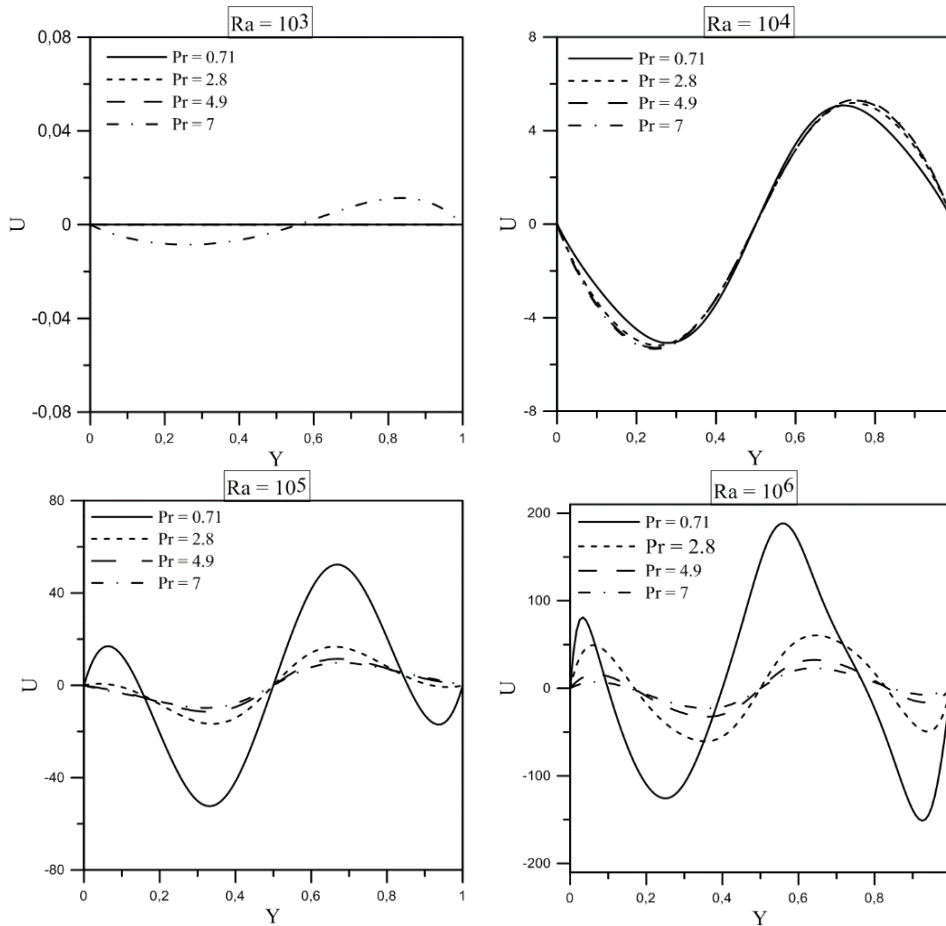


Figure 5: Horizontal velocity in the middle of the cavity ($X = 0.5, Y = 0$ to 1) for various Rayleigh and Prandtl numbers

In the middle of the wall ($0.25 \leq Y \leq 0.75$) the profiles of local Nusselt undergo a decreasing evolution and heat transfer by natural convection becomes important. Therefore, the heat transfer is less pronounced along this area by increasing Prandtl number.

When $Ra = 10^6$, the local Nusselt number decreases along the hot wall, especially for $Pr \geq 2.8$. At $Pr = 0.71$, the profile of local Nusselt number follow a slight increase at the

bottom of the wall to reach a critical value then decrease along the rest of the wall. The Nusselt number is less pronounced along the hot wall by increasing the Prandtl number and the heat transfer corresponds to a natural convection for great values of the Rayleigh number. However, for the large temperature gradients, heat transfer seems invariant when $Pr \geq 4.9$ and local Nusselt number profiles remain constant.

Figure 7 illustrate the heat transfer given by the average Nusselt number for different values of Rayleigh ($Ra = 10^3$ to 10^6) and Prandtl ($Pr = 0.71$ to 7). It is evident to note that the heat transfer increases significantly when the Rayleigh number increase and, particularly, for of very high Rayleigh numbers. For low temperature gradients, the heat transfer is not affected by the Prandtl number variations. Both average Nusselt profiles for $Ra = 10^3$ and 10^4 follow constant evolution according to Prandtl number. At $Ra = 10^5$ and 10^6 , significant improvement in heat transfer is noted. However, for very high values of the Rayleigh number, the average Nusselt number undergoes an approximately constant decrease when Prandtl increases, indeed, the heat transfer is less pronounced with increasing Prandtl.

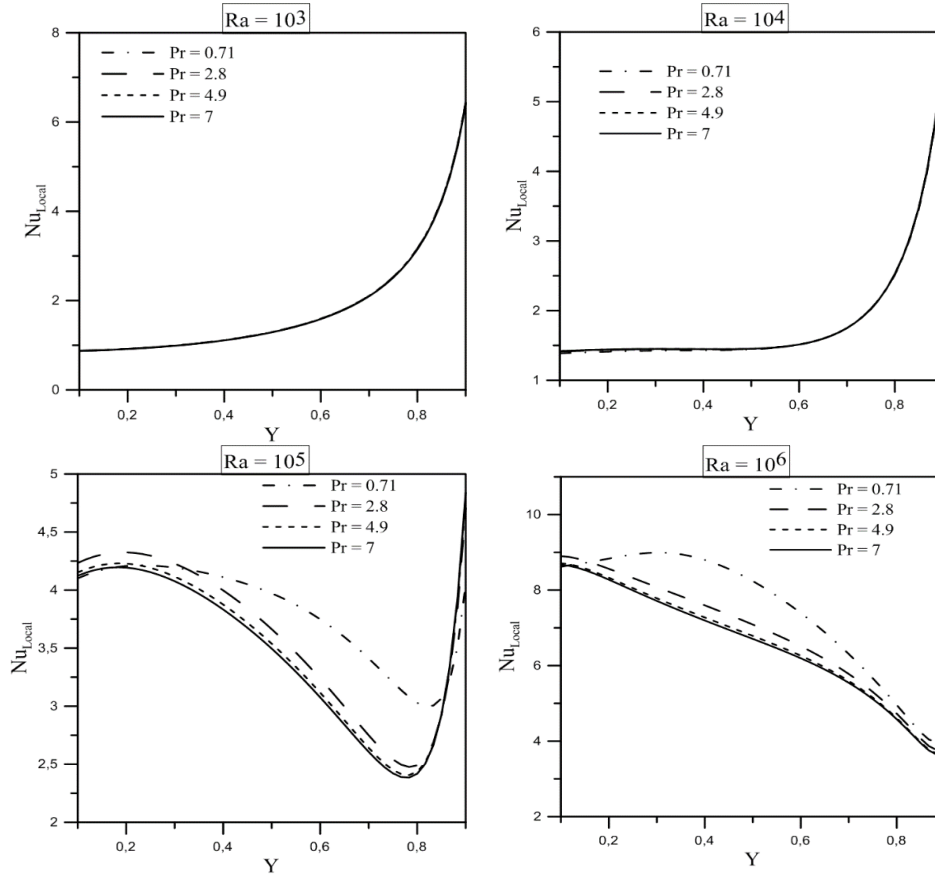


Figure 6: The local Nusselt number at the hot wall for various Rayleigh and Prandtl numbers

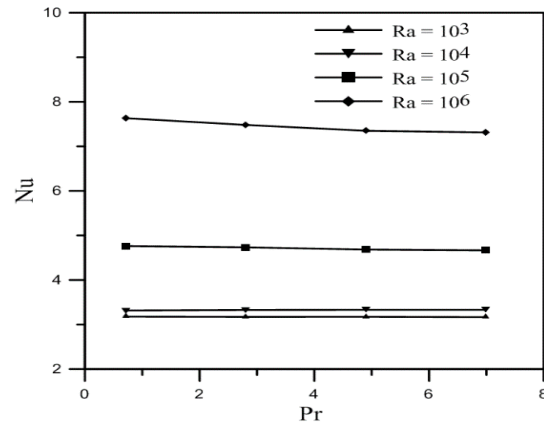


Figure 7: The average Nusselt number at hot side walls versus Prandtl number for various Rayleigh numbers

5 Conclusions

In this work a numerical study of the steady natural convection in a square cavity subject to the boundary conditions on the side walls is performed. The fluid considered is Newtonian. The equations governing the flow and heat transfer are given in dimensionless form. The finite volume method was adopted to solve the algebraic system. The setting in dimensionless form of the governing equations brings up the dimensionless numbers, namely the Rayleigh and the Prandtl numbers. In order to see the influence of these numbers on the flow field and the heat transfer, the review was done for different values of Ra and Pr.

The results indicate that:

- The heat transfer and flow field are more pronounced with increasing Rayleigh number and the thermal boundary layer tends to grow towards the side walls for very high Rayleigh numbers.
- At low Rayleigh numbers, the flow field is slightly pronounced with increasing Prandtl number and decreases by increasing the Rayleigh number, as well as the heat transfer is not affected by variations of Prandtl number for low Rayleigh numbers and, is less pronounced by increasing the Prandtl number for very high Rayleigh numbers.

References

- Aminossadati, S.M.; Ghasemi, B.; Kargar, A.** (2014): Computational analysis of magnetohydrodynamic natural convection in a square cavity with a thin fin. *European Journal of Mechanics B/Fluids*, vol. 46, pp.154–163.
- Basak, B.; Roy, S.; Balakrishnan, A.R.** (2006): Effects of thermal boundary conditions on natural convection flows within a square cavity. *International Journal of Heat and Mass Transfer*, vol.49, pp. 4525–4535.

Bejan, A.; Georgiadis, J. G. (1992): The Prandtl number effect near the onset of Bénard convection in a porous medium. *International Journal of Heat and Fluid Flow*, vol. 13, No. 4.

Chandra, A.; R. P. Chhabra, R. P. (2012): Effect of Prandtl Number on Natural Convection Heat Transfer from a Heated Semi-Circular Cylinder. *World Academy of Science, Engineering and Technology*, vol. 6, pp. 01-29.

Cianfrini, C.; Corcione, M.; Dell’Omo, P, P. (2005): Natural convection in tilted square cavities with differentially heated opposite walls. *International Journal of Thermal Sciences*, vol. 44, pp. 441–451.

Corcione, M. (2003): Effects of thermal boundary conditions at the sidewalls, upon natural convection in rectangular enclosures heated from below and cooled from above. *International Journal of Thermal Sciences*, vol. 42, pp. 199-208.

De Vahl Davies, G. (1968): Laminar Natural convection in an enclosed rectangular cavity. *International Journal of Heat Mass Transfer*, vol. 11, pp. 1675-1693.

De Vahl Davies, G. (1983): Natural convection of air in a square cavity a bench mark numerical solution. *International Journal of numerical Methods of fluids*, vol. 3, pp. 249–264.

Hinojosa, J. F.; Cervantes-de Gortari, J. (2010): Numerical simulation of steady- state and transient natural convection in an isothermal open cubic cavity. *Heat and Mass Transfer*, vol. 46, pp. 595-606.

Hortmann, M.; Peric, M.; Scheuerer, G. (1990), Finite volume multigrid prediction of laminar natural convection: bench-mark solutions. *International Journal Numerical Methods in Fluids*, vol. 11, pp. 189–207.

Huelez, G.; Rechtman, R. (2013): Heat transfer due to natural convection in an inclined cavity using the Lattice Boltzman equation method. *International Journal of Thermal Sciences*, vol. 65, pp. 111-119.

Koca, A.; Oztop, H, F.; Varol, Y. (2007): The effects of Prandtl number on natural convection in triangular enclosures with localized heating from below. *International Communications in Heat and Mass Transfer*, vol. 34, pp. 511–519.

Lage, J. L.; Bejan, A.; Georgiadis, J. (1991): On the effect of the Prandtl number on the onset of Bénard convection. *International Journal of Heat and Fluid Flow*, vol. 12, No. 2.

Mahmoudi, M. (2011): Numerical simulation of free convection of nanofluid in a square cavity with an inside heater. *International Journal of Thermal Sciences*, vol. 50, pp. 2161-2175.

Mahmoudi, A.; Mejri, I.; Abassi, M. A.; Omri, A. (2013): Numerical Study of Natural Convection in an Inclined Triangular Cavity for Different Thermal Boundary Conditions: Application of the Lattice Boltzmann Method. *FDMP: Fluid Dynamics & Materials Processing*, vol. 9, no. 4, pp. 353-388.

Misici, L. (1984): Natural Laminar convection in Rectangular cavity, an analytic solution, *MECCANICA*, vol. 19, pp. 111-115.

Montiel, G. M.; Hinojosa, J. F.; Villafan, V. H. I.; Bautista, A. O.; Estrada, C. A. (2015): Theoretical and experimental study of natural convection with surface thermal radiation in a side open cavity. *Applied Thermal Engineering*, vol. 75, pp. 1176-1186.

Nardini, G.; Paroncini, M. (2012): Heat transfer experiment on natural convection in a square cavity with discrete sources. *Heat and Mass Transfer*, vol. 48, pp. 1855-1865.

Oztop, F.; Zaiguo, F.; Bo, Y.; Wei, J. (2011): Conjugate natural convection in air filled tube inserted a square cavity. *International Communications in Heat and Mass Transfer*, vol. 38, pp. 590–596.

Patankar, S. V. (1980): *Numerical Heat Transfer and Fluid Flow*, Hemisphere Published, New York.

Pesso, T.; Piva, S. (2009): Laminar natural in a square cavity: Low Prandtl and large density differences. *International Journal of Heat and Mass Transfer*, vol. 52, pp. 1036–1043.

Poujol, F.T.; Rojas, J.; Ramos, E. (2000) Natural convection of a high Prandtl number fluid in a cavity, *International Communications in Heat and Mass Transfer*, vol. 27, pp. 109–118.

Sadaou, D.; Sahi, A.; Hamici, N.; Meziani, B.; Amoura, T. (2015): Free convection in a square enclosure with a finned plate. *Mechanics & Industry*, vol. 16, no. 3.

Yoo, J. S. (1999): Prandtl number effect on transition of free-convective flows in a wide-gap horizontal annulus, *International Communications in Heat and Mass Transfer*, vol. 26, pp. 811–817.